RESEARCH ARTICLE
SOLID EARTH: SEISMOLOGY

Earth and Planetary Physics
1: 26-34, 2017
doi: 10.26464/epp2017004

A seismic model for crustal structure in North China Craton

TianYu Zheng[1*], YongHong Duan[2], WeiWei Xu[3], and YinShuang Ai[1]

[1]Key Laboratory of Earth and Planetary Physics, Institute of Geology and Geophysics, Chinese Academy of Sciences, Beijing 100029, China;
[2]Geophysical Exploration Center, China Earthquake Administration, Zhengzhou 450002, China;
[3]Institute of Geophysics, China Earthquake Administration, Beijing 100081, China

Abstract: We present a digital crustal model in North China Craton (NCC). The construction of crustal model is based on digitization of original seismic sounding profiles, and new results of three-dimensional structure images of receiver functions. The crustal model includes seismic velocity and thickness of crustal layers. The depths to Moho indicate a thinning crust ~30 km in the east areas and a general westward deepening to more than 40 km in the west. The P wave velocity varies from 2.0 to 5.6 km/s in the sedimentary cover, from 5.8 to 6.4 km/s in the upper crust, and from 6.5 to 7.0 km/s in the lower crust. By analyzing regional trends in crustal structure and links to tectonic evolution illustrated by typical profiles, we conclude that: (1) The delimited area by the shallowing Moho in the eastern NCC represents the spatial range of the craton destruction. The present structure of the eastern NCC crust retains the tectonic information about craton destruction by extension and magmatism; (2) The tectonic activities of the craton destruction have modified the crustal structure of the convergence boundaries at the northern and southern margin of the NCC; (3) The Ordos terrene may represent a relatively stable tectonic feature in the NCC, but with the tectonic remnant of the continental collision during the assembly of the NCC in the north-east area and the response to the lateral expansion of the Tibetan Plateau during the Cenozoic in the south-west.

Keywords: crustal velocity model; Moho; sedimentary cover; tectonic evolution; North China Craton

Citation: Zheng, T. Y., Y. H. Duan, W. W. Xu, and Y. S. Ai (2017). A seismic model for crustal structure in North China Craton. *Earth Planet. Phys.*, *1*, 26-34. http://doi.org/10.26464/epp2017004

1. Introduction

Stable cratons are the most important tectonic elements of the continental lithosphere. Thus, their evolution is of substantial importance for understanding the whole Earth's dynamic system. Only the cratons carry the information about the Earth's dynamic processes in the Precambrian. Moreover, long-term evolution, especially, cratonic destruction is crucial for distinguishing between regional perturbations and precursors to continental dispersal.

The North China craton (NCC) is one of the world's oldest cratons, and was tectonically stable in the Paleozoic. From the Late Mesozoic to the Cenozoic, the eastern NCC has experienced significant tectonic reactivation, which results in the total loss of craton stability due to changes in the physical and chemical properties of the lithosphere of involved craton (Zhu RX et al., 2012). However, the western NCC (Ordos terrene) remained tectonically stable during the long-term evolution of the NCC (Qiu RZ et al., 2004; Zhai MG, 2008). The NCC consists of a relatively intact western part and a destroyed eastern part, and thus can be considered as a typical example to study the continental geodynamics. Geophysical surveys provide such an opportunity to construct a fine-scale structure of the present crust and mantle.

Correspondence to: T. Y. Zheng, tyzheng@mail.igcas.ac.cn
Received 28 APR 2017; Accepted 08 JUN 2017.
Accepted article online 17 AUG 2017.

Seismic observations covering the entire NCC provided basic data for probing the crust structure of the NCC. We constructed a three-dimensional (3D) digital crustal velocity model in the NCC as a part of the Crust and Upper Mantle Velocity Model of North China (VMNC), named C-VMNC, and published it online (http://www.craton.cn/data [2017-03-01]). This study presents the results of C-VMNC on the structure of the crust. The parameters of crustal model included seismic wave velocity *V*p (and /or *V*s) and thickness (depth of velocity discontinuity) of crustal layers. According to the data coverage and the tectonic characteristics in the NCC, we used different seismic imaging technique to construct the crustal model in different region, respectively. In the eastern NCC the two-dimension (2D) imaging results of seismic wide-angle reflection/refraction profiling were compiled into 3D crustal model. In the western and northern NCC, the receiver function imaging was used to construct the 3D crustal model. This database is used to review and analyze the seismic velocity structures of the crust in this study.

2. Tectonic Evolution: An Overview

The NCC is one of the world's oldest cratons. This craton preserves continental rocks as old as 3.8 Ga (Liu DY et al., 1992). The basement of the NCC consists of variably exposed Archean-Paleoproterozoic rocks in the northern and central orogens (Zhao GC et al., 2001). Based on the field relations and geochronological data of the exposed metamorphic rocks, the Paleoproterozoic subduction-accretion-collision tectonics of the NCC was elucidated (Zhao

GC et al., 2001; Zhai MG and Santosh, 2011; Guo JH et al., 2012; Peng P et al., 2015). In the Late Archean to Early Paleoproterozoic, continued subduction led to the formation of island and magmatic arcs, and resulted in a major continent-continent collision between the eastern and western blocks and the final amalgamation of the NCC ~1.85 Ga. The basement of the NCC was subsequently covered by thick sequences of Mesoproterozoic to Neoproterozoic and Paleozoic sediments. Igneous activity was weak in the Paleozoic, which implies that the NCC was tectonically stable during that time (Wang HZ and Mo XX, 1995).

As a terrane derived from eastern Gondwana margin the NCC and South China Block rifted and separated from Gondwana with the successive opening and closure of the Palaeo-Tethys in the Devonian (Metcalfe, 2011). The northwards drift of the Gondwana-derived continental terranes, and continent assemblage of continental terranes settled the NCC into the East Asia. To the north, amalgamations of the NCC with the accretion terranes of the Central Asian Orogen occurred during the Late Permian to Early Triassic, after the paleo-oceanic lithosphere had subducted beneath the northern margin of the NCC along the Solonker suture zone (Xiao WJ et al., 2003). To the south, the continent-continent collision between the NCC and the Yangtze craton was one of the most important accretion events. The Qinling Orogen represents a convergence boundary where the Yangtze craton subducted northward beneath the NCC in the Triassic (Meng QR and Zhang GW, 2000).

Since the Late Mesozoic, the NCC has become an important active part of the circum-Pacific tectonomagmatic zone. Mesozoic igneous rocks are widespread in the eastern NCC, and are accompanied by metamorphic core complexes and extensional basins (Wu FY et al., 2005; Darby et al., 2004; Ren JY et al., 2002). A comparison of the Paleozoic kimberlite borne and Cenozoic basalt-borne mantle xenoliths indicates that the thick, cold, and refractory Archean lithospheric mantle beneath the eastern NCC has been removed and replaced by the thin, hot, and relatively fertile juvenile lithospheric mantle (Fan W and Menzies, 1992; Menzies et al., 1993). These lines of evidence indicate that the eastern NCC has experienced significant tectonic reactivation from the late Mesozoic to the Cenozoic, which results in the total loss of craton stability due to changes in the physical and chemical properties of the lithosphere of involved craton (Zhu RX et al., 2012).

The Ordos terrane in the western NCC remained tectonically stable during the long-term evolution of the NCC. Despite no outcrops within Ordos, the geophysical surveys across the Ordos demonstrate that Ordos has the characteristics of stable continent, namely low heat flow, low seismicity, a crust that is more than 40 km thick, and a lithosphere that is locally up to 200-250 km thick and has experienced little deformation except around its edges since the Precambrian (Qiu RZ et al., 2004; Zhai MG, 2008).

3. Seismic Data Coverage and Methodology

An enormous quantity of high-fidelity seismic recordings has been collected at densely distributed stations. The data obtained from the very intensive seismic observations in the NCC have enabled the study of crustal structures in unprecedented detail and the construction of a 3D crustal velocity model. The permanent stations installed by the China National Seismic Network (CNSN) (e.g., Zheng XF et al., 2010) exist over the eastern NCC (Figure 1), in which most stations are equipped with broad-band sensors, whereas the stations in the basin area are equipped with short-period sensors. The seismic station coverage is sparse in the western Ordos terrane. The broadband portable seismic experiments were performed between 2001 to 2011 as parts of the North China Interior Structure Project (NCISP) and the Destruction of the North China Craton (DNCC) project (e.g., Zhu RX et al., 2012). A total of 534 temporary stations equipped with portable broadband seismometers in 8 profiles (NCISP1-8) with an average spacing of about 10-15 km and two 2-D seismic temporary arrays (Wang CY et al., 2014) have been deployed that span major tectonic units in the NCC (Figure 1). Recently, the public available seismic data from many permanent and temporary seismic arrays produce a high-quality, dense, and homogenous data set.

The improvements in station coverage and receiver function method enable more detailed imaging of the structure in the NCC. Along the observed profiles the crust of continental NCC has been studied in detail. Details of the development of crustal studies may be found in published papers (e.g. http://www.craton.cn/data [2017-03-01]). However, it is questionable to image the crustal structure using receiver function method in the eastern NCC, in which the major area is covered by thick Cenozoic sediments. Identifying the P-to-S phases converted from the velocity discontinuities in crust and upper mantle is essential for reliable structural imaging in the receiver function method. The presence of thick sediments, however, makes the recognition of the expected phases rather difficult and leaves great uncertainty in the resultant images, due to heavy interference of strong sediment reverberations with the converted phases produced at deeper discontinuities.

A dense network of deep seismic sounding profiles existed over the eastern NCC, especially the capital area (Duan YH et al., 2016). From 1976 to 2011, 52 deep seismic sounding profiles were completed over different periods (Figure 2). In the capital region, profiles have been created at a distance of about 30-50 km from each other, with the density of the profiles gradually reducing in the surrounding area. Three long wide-angle reflection/refraction profilings, as part of the DNCC, were performed with a total length of 3400 km (Duan YH et al., 2016). The combined ocean-bottom-seismometer and land portable seismometer survey was carried out in the Bohai region along two profiles with a total length of ~930 km (Liu LH et al., 2015). These deep seismic sounding profiles provided the dense data coverage to explore the crustal structure of the eastern NCC and build a 3D crustal velocity model of the eastern NCC.

According to the tectonic characteristics and the data coverage, we constructed a 3D crustal velocity model using receiver function imaging in the western NCC, and by interpolating seismic wide-angle reflection/refraction profiling results in the eastern NCC, respectively. The 3D model C-VMNC is constructed based on the data: (1) 45 seismic wide-angle reflection/refraction profiles performed from 1976 to 2011 (Figure 2); (2) teleseismic records from 681 temporal seismic stations between 2000 to 2011 (Figure 1); (3) teleseismic records from 370 stations of CNSN between 2011 to 2013 (Figure 1).

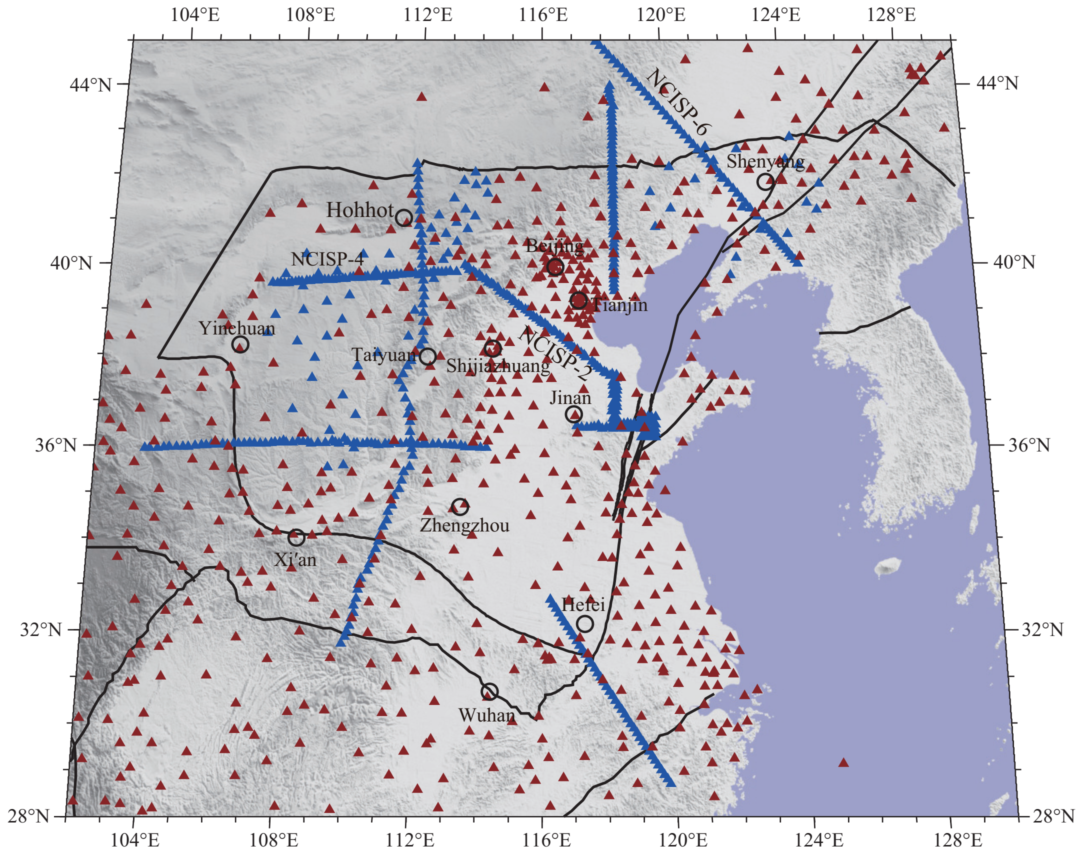

Figure 1. Map of the seismic stations and seismic observation profiles in the NCC and adjacent region with the boundary of the North China craton and Yangtze craton (black lines). Blue triangles represent temporary seismic stations; amaranth triangles represent Chinese National Digital Seismic Network stations. The names of the observation profiles used in the text and in Figures 7 and 8 are marked.

In the eastern NCC (36°-42°N, 112°-120°E), Duan YH et al. (2016) collected 45 seismic wide-angle reflection/refraction 2-D profiling results and performed gridding of the velocity and interface depth data by using the Kriging interpolation method. The 3D model was constructed from the velocity structure of 2D controlling section. The horizontal meshing of the model is 0.25°×0.25°. The velocity and interface are gridded at an interval of 5 km in the horizontal direction, and 1 km and 2 km above and below 10 km respectively in the vertical direction in the controlling sections. The parameters of the 3D model include (1) the thickness of the sedimentary cover (depth to the basement); (2) the interface depth between upper crust and lower crust; (3) the depth to Moho, (4) the average seismic velocity in sedimentary layer, upper crust, and lower crustal respectively.

In the western region (34°-40°N, 104°-114°E) and northern margin (40°-42°N, 108°-129°E) of the NCC, the receiver function imaging method was used to construct the 3D crustal model. To explore the 3D crustal structure, we used a wavefield reconstruction method (Zhang JH and Zheng TY, 2015) to accurately map teleseismic data from a sparsely spaced seismic network. The acquired regular and fine-scale observation system has a uniform spacing of 0.2°×0.2° in both the west-east and north-south directions. We inferred 3D variations in the shear wave speed in the crust using a velocity structure imaging technique for receiver functions (Zheng TY et al., 2015) based on the regularized data. The 3D model was built from one-dimension models parameterized as a stack of layers beneath each virtual receiver. The model parameters include shear wave velocity *Vs*, thickness, and *Vp*/*Vs* in each layer. The thickness of the sedimentary cover, the interface depth between upper crust and lower crust, and the depth to Moho are acquired from the model parameters.

4. Regional Trends in Crustal Structure and Links to Tectonic Evolution

The database of C-VMNC consists of a 3D digital crustal velocity model and structural models of the typical profiles collected from previous published results. In the model, four layers are divided by three interfaces: between the sedimentary cover and crystalline crust, the upper and lower crust, and the crust and upper mantle. In the eastern NCC, the wave velocities were estimated by the deep seismic sounding profile. In the sedimentary cover, the surface velocity varies widely from 2.0 to 5.6 km/s, and the value gradually increases to 5.0-5.8 km/s downward with a positive gradient. The upper crust has the velocity of 5.8 to 6.4 km/s. The velocity of the lower crust generally ranges from 6.5 to 7.0 km/s. Velocity at the top of the mantle generally ranges from 7.9 to 8.0 km/s. The absolute wave velocities cannot be determined directly using receiver function imaging, in the western NCC. A reasonable estimation was achieved based on the clearly inferred crustal layering, and the ranges of the permissible wave velocities estim-

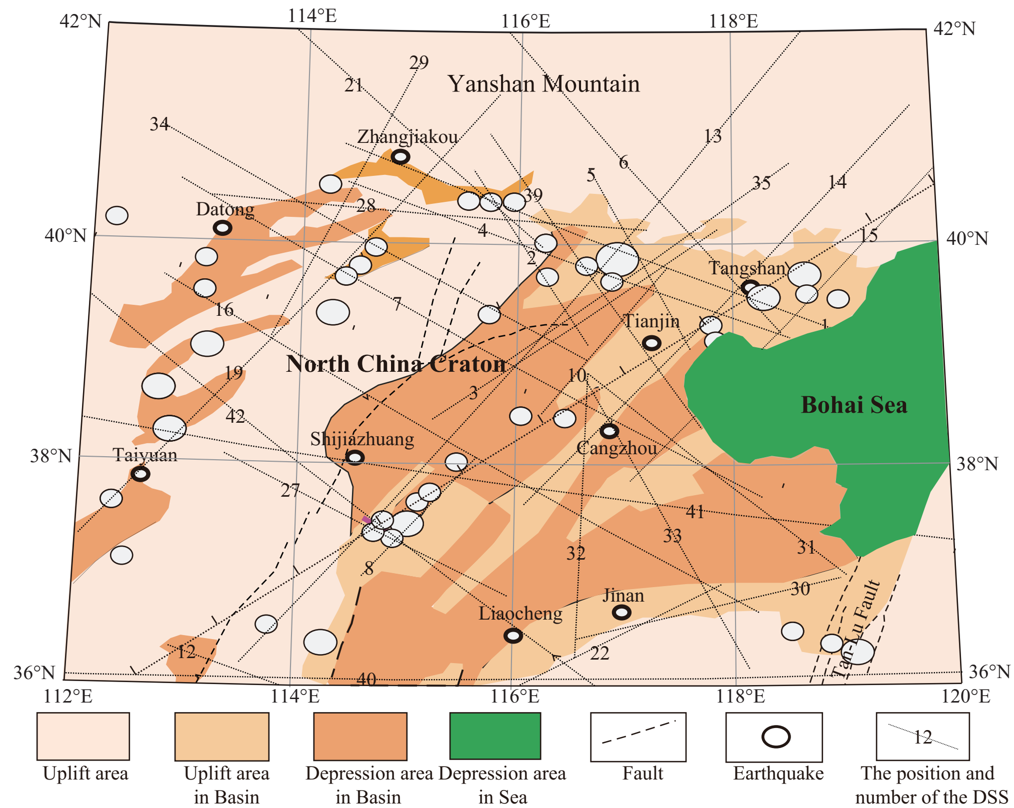

Figure 2. Position of DSS profiles (black lines with the number of profile) in the study area showing simplified tectonic setting. The name of profiles is listed in the next. 1.Luoting-Zhangjiakou; 2. Yanshan-Daxing-Yanqing; 3. Anguo-Yongqing-Zhunhua; 4. Ninghe-Beijing-Zhuolu; 5. Tanggu-Sanhe-Miyun; 6. Bogezhuang-Fengning-Zhenglan Qi; 7. Haixing-Yangyuan-Fengzhen; 8. Renxian-Hejian-Wuqing; 10. Hejian-Wuqing; 12. Heze-Linzhou-Changzhi 13. Shijiazhuang-Kalaqin Qi; 14. Cangzhou-Tianjin-Kalaqin Qi; 15. Dezhou-Qinhuangdao; 16. Zhucheng-Dingxian-Tuoketuo; 19. Taiyuan-Xuanhua; 21. Beijing-Zhangjiakou-Huade; 22. Zhengzhou-Jinan; 27. Tai'an-Longyao-Xinxian; 28. Beijing-Huailai-Fengzhen; 29. Fanshi-Huai'an-Taibus Qi; 30. Qihe-Zhangqiu-Shouguang; 31. Shouguang-Zhanhua-Wen'an; 32. Wen'an-Dezhou-Qihe; 33. Xinyuan-Leling-Dacheng; 34. Wen'an-Yuxian-Chayouzhong Qi; 35. Anxin-Xianghe-Kuancheng; 39. Tianjin-Beijing-Chicheng; 40. Zhucheng-Yichuan; 41. Wendeng-Alxa; 42. Yancheng-Baotou.

ated from deep seismic sounding studies (Liu MJ et al., 2006; Jia SX et al., 2014). The sedimentary cover has the velocity ranging from 5.1 to 5.8 km/s, and with the surface velocity of 4.4 to 4.7 km/s. The velocity generally ranges from 6.0 to 6.3 km/s in the upper crust, and from 6.5 to 6.9 km/s in the lower crust. The velocity of the crust-mantle zone varies from 7.0 to 7.4 km/s. As the examples, Figure 3 shows the velocity structure from the slices of the 3D model at 35°, 38°, and 40°. All of the slices of the 3D model at an interval of 1° were published online (http://www.craton.cn/data[2017-03-01]).

We give a brief discussion of the crustal structure for major tectonic provinces in the NCC based on the topography of the depth to Moho (Figure 4) and the map of the thickness of sedimentary cover (Figure 5) from the C-VMNC. Then we review and analyze the "frozen-in" tectonic information in the crust based on the seismic velocity structure of the crust from typical profiles.

The topography of the depth to Moho based on the database of the C-VMNC is illustrated in Figure 4. Major observations from the map of the Moho depth indicate a thin crust ~30 km in the east area and a general westward deepening to more than 40 km in the west in the NCC. Near the boundary between the eastern and central NCC, a rapid thickness variation of crust is observed and is roughly coincident with the North-South Gravity Lineament. The tectonic regime in the NCC changed from the north-south partition to the east-west partition during Mesozoic time (Wang HZ and Mo XX, 1995). The east-west trend of observed change of the depth to Moho in the NCC thus indicates that the present structure of the NCC crust represents a tectonic remnant corresponding to craton destruction during the Late Mesozoic to Cenozoic. The structural pattern of east-west partition also implies that the tectonic activities of the craton destruction have modified the crustal structure of the convergence boundaries at the northern and the southern margin of the NCC.

To make a general survey of the Moho topography in the NCC and its adjacencies, the delimited area by the shallowing Moho represents the spatial range of the cratonic destruction. The thickened crust of ~ 60 km in the south west of the Ordos can be ascribed to the response to the lateral expansion of the northeastern Tibetan Plateau derived from the India-Asia collision during the Cenozoic. The crustal root beneath the northeastern Ordos terrene is considered as a tectonic remnant of the continental collision during the assembly of the NCC in the Paleoproterozoic (Zheng TY et al., 2009).

The thickness of sedimentary strata, as revealed by seismic ima-

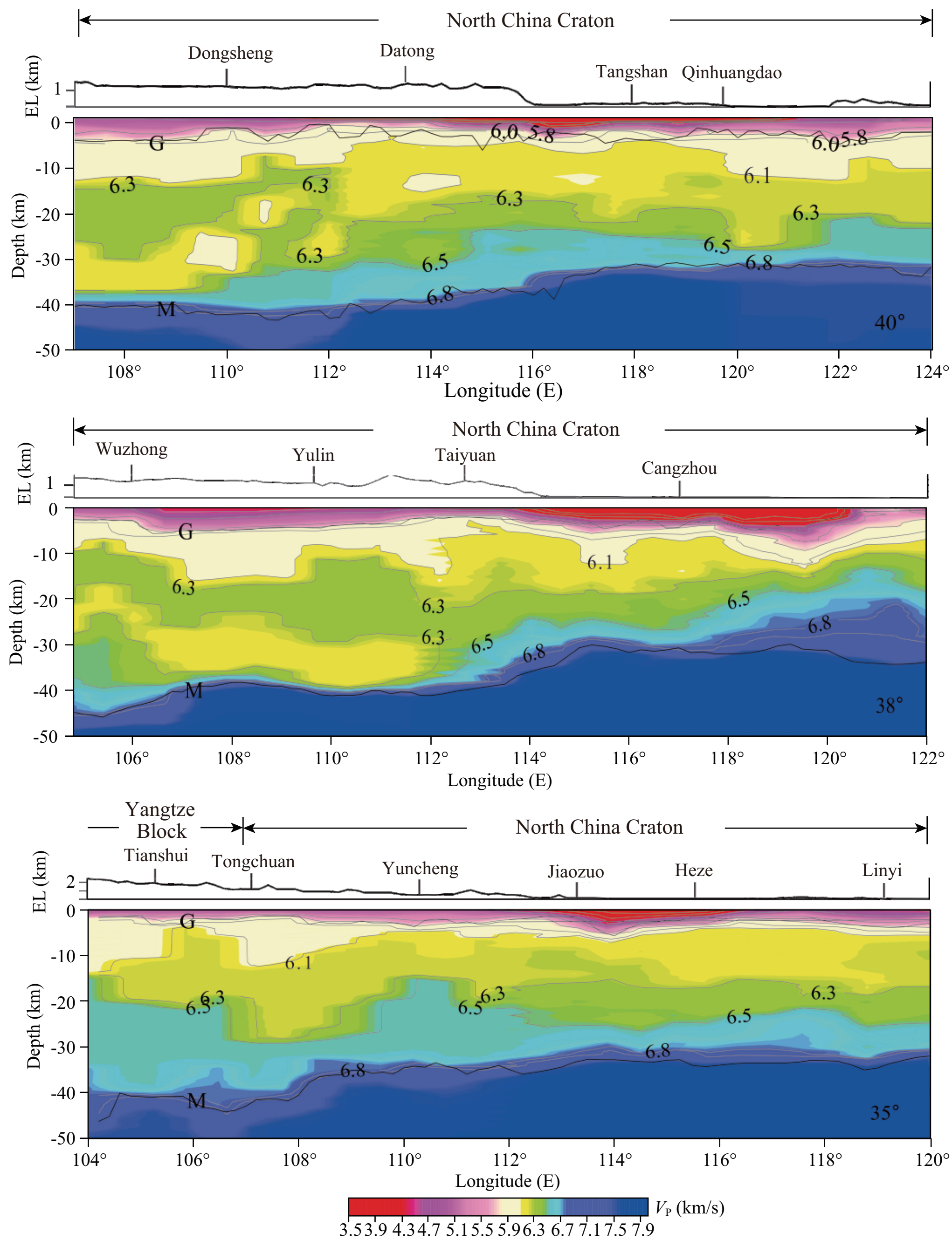

Figure 3. Cross slices of the 3D crustal velocity structure model of the C-VMNC at 35°, 38°, and 40° in the North China Craton. The scale of P wave velocity is shown on the bottom, and the velocity values (km/s) are marked in the diagram.

ging from the database of the C-VMNC, is illustrated in Figure 5. The structure of the cover can be distinguished into the basin group in the east, the Ordos basin in the west, and the graben system around the Ordos (Figure 5). An important geological record for the NCC destruction is widespread Early Cretaceous extensional or rifted basins. Several basin groups, each consisting of a series of medium- to small-scale basins, dominate the eastern NCC. As shown in Figure 5, they include a northern group in the Yinshan tectonic belt and southern margin of the Songliao Basin, a middle group around Bohai Bay and along the eastern margin of the Taihang Mountains, and a southern group consisting of the Hefei and Zhoukou basins. The structure of sedimentary cover in the eastern NCC indicates crustal modification by extension and magmatism.

In contrast to the wide rift basins in the eastern NCC, the Ordos basin developed into a major depression basin deepening westward. The uniform sedimentary strata indicate that no obvious crustal modification resulting from extension and magmatism occurred in the western NCC since the Paleozoic. Around the Ordos terrene, the thickness of the cover in the graben system, consisting of the Yinchuan graben, Hetao graben, Shanxi graben, and Weihe graben, is variable and with outcrops of basement rocks in

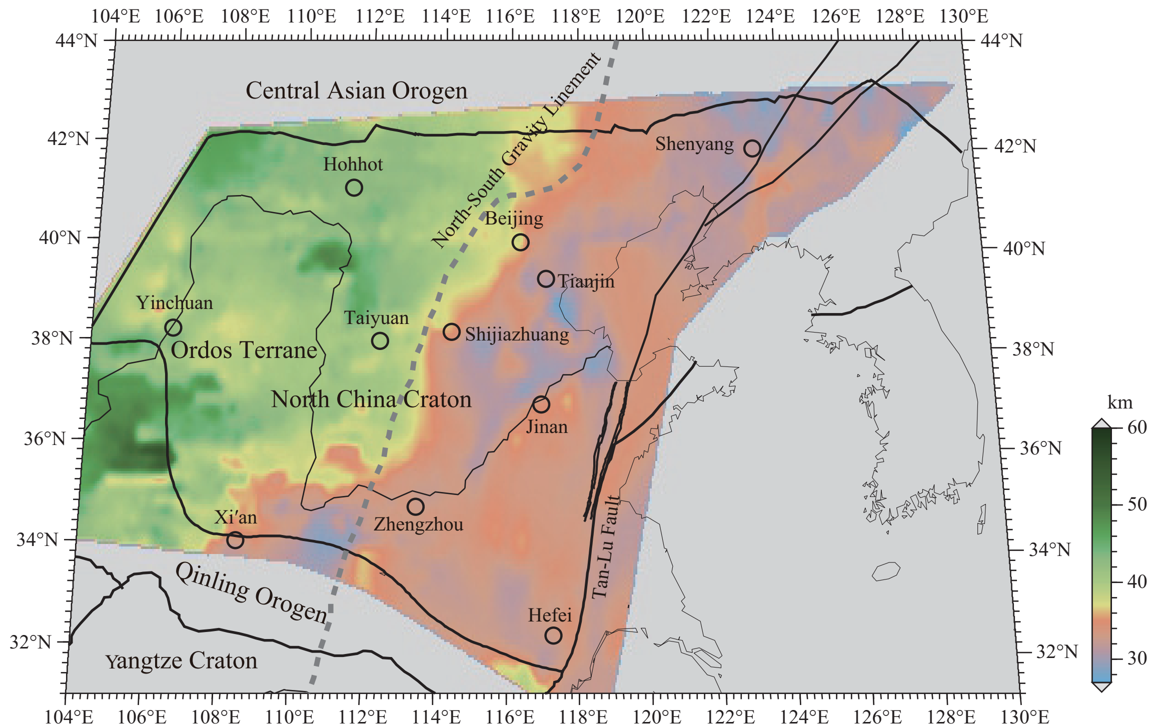

Figure 4. Topography of depth to Moho (km) based on the database of the C-VMNC. Black thick lines represent the boundary of North China craton and Yangtze craton; gray dashed line represents the North-South Gravity Lineament. The scale of depth is shown at the right.

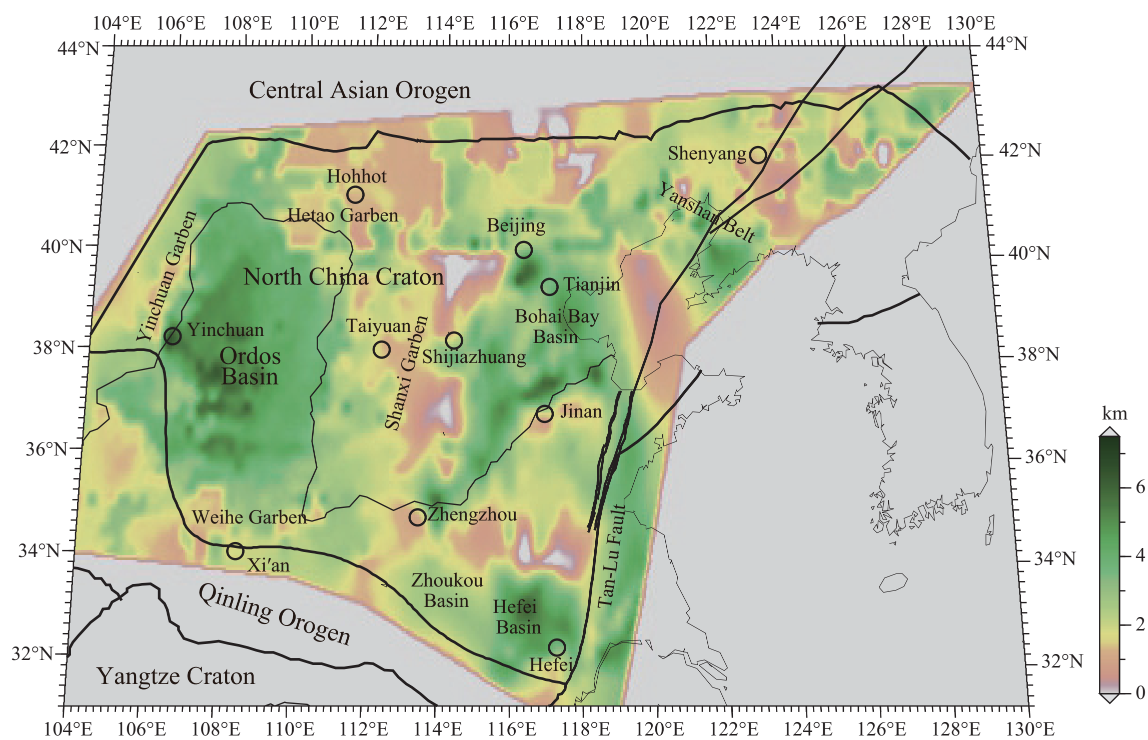

Figure 5. Thickness of sediments (km) based on the database of the C-VMNC. Black thick lines represent the boundary of North China craton and Yangtze craton. The scale of thickness is shown at the right.

local areas. The structural pattern, that a graben system with various shallow structure surrounding the ancient stable craton terrene, suggests a difference in shallow tectonic evolution in the Cenozoic time after craton destruction.

The complexities and varieties of the crust interior structure in the NCC are observably displayed in the reconstructed crustal velocity model in the seismic observation profiles. These seismic imaging results of typical profiles are collected in the VMNC (http://www.

craton.cn/data [2017-03-01]). The “frozen-in” information in the crust would improve our understanding of cratonic formation and long-term evolution since Archean and the cratonic destruction during Mesozoic-Cenozoic. We show and review three profiles of them in the next.

The P-wave velocity image of the Yancheng-Baotou profile (Figure 6) was obtained from the seismic wide-angle reflection/refraction profiling (Duan YH et al., 2015). The results indicated significant differences between the lithospheric structures in the east and west of the Taihang Mountains. The Bohaiwan Basin has a very thick Cenozoic sedimentary cover and the deepest point of crystalline basement is about 7.0 km, with the crustal thickness decreasing to about 31.0 km. The crystalline basement of the Luxi uplift zone is relatively shallow with a depth of 1.0-2.0 km and crustal thickness of 33.0-35.0 km. The Subei Basin has a thicker Cenozoic sedimentary cover and the bottom of its crystalline basement is at about 5.0-6.0 km with a crustal thickness of 31.0-32.0 km. The Tanlu fault is a deep fracture which cuts the lithosphere with a significant velocity structure difference on either side of the fault. The formation of the contrasting structure is attributable to one of two possibilities: the trans-lithospheric Tanlu fault zone operated as an asthenospheric upwelling channel and facilitated the NCC reactivation, or the Tanlu fault zone separates the study region into two lithospheric blocks, with the ancient lithospheric materials remaining within the rejuvenated lithospheric mantle (Zheng TY et al., 2008). West of the Taihang Mountains, the crustal thickness increases significantly. The crust thickness beneath the Shanxi fault depression zone is about 46 km, and there is a low-velocity structure with a velocity of less than 6.1 km/s in the upper part of the middle crust.

The seismic wide-angle reflection/refraction profiling constrains the values of wave velocity well, and the receiver function imaging improves the recognition of structural fabric by distinguishing the velocity discontinuity. The crustal shear wave velocity structure along the Lijin-Datong-Etuoke profile, crossing the NCC in E-W direction (Figure 7), was compiled from the velocity mod-

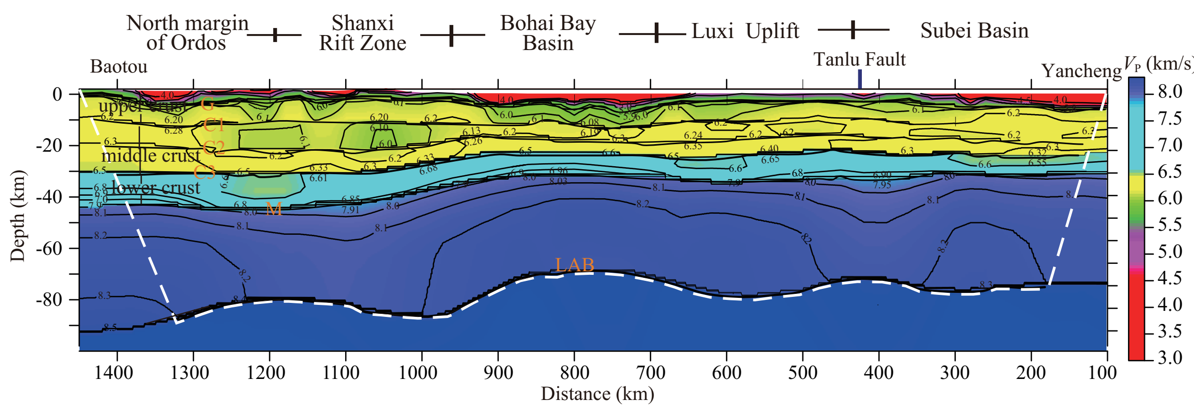

Figure 6. Lithospheric velocity structure from the Yancheng-Baotou deep seismic profiling (modified from Duan YH et al., 2015). The scale of P wave velocity is shown on the right and the velocity values (km/s) are marked in the diagram. G: basement interface; M: Moho; LAB: Lithosphere-asthenosphere boundary.

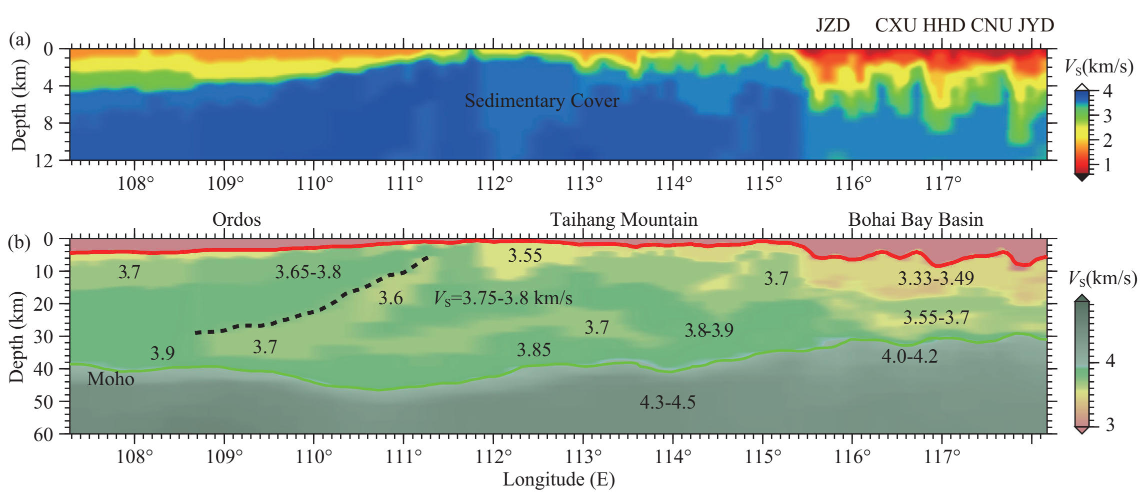

Figure 7. Cross section of the shear-wave velocity structure based on receiver function imaging along the seismic observation profiles NCISP-2 and NCISP-4 with E-W trending (data from Zheng TY et al., 2006, 2009). (a) Sedimentary structure; (b) crustal structure with marked velocity values (km/s). The scale of S velocity is shown on the right. CNU: Chengning Uplift; CXU: Cangxian Uplift; HHD: Huanghua Depression; JYD: Jiyang Depression; JZD: Jizhong Depression.

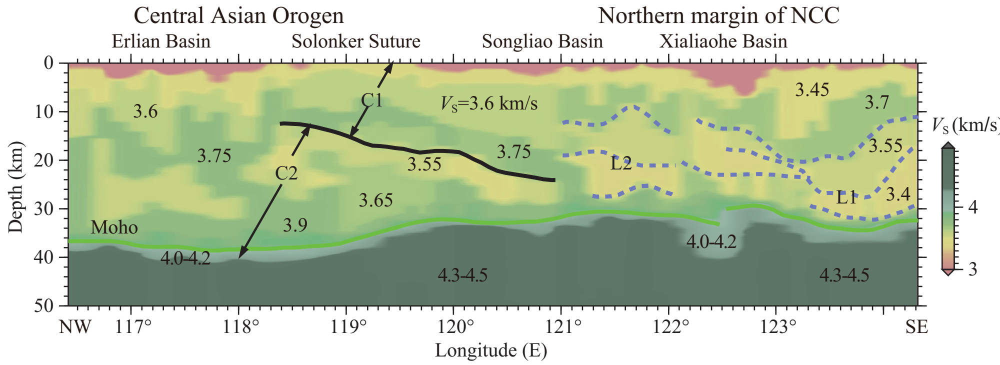

Figure 8. Cross section of the shear-wave velocity structure based on the receiver function imaging along the NCISP-6 profile (data from Zheng TY et al., 2015). The scale of S velocity is shown on the right and the velocity values (km/s) are marked in the diagram. The blue dashed lines mark the velocity discontinuities, and the dark line represents the boundary between C1 and C2. In the northeastern margin of the NCC, low-velocity zones L1 and L2 occupy most of the space in the depth range of approximately 10–30 km and present shear velocities of 3.4 km/s and 3.55 km/s and inversion velocity discontinuities. Beneath the Central Asian Orogenic Belt, the velocity structures are characterized by superimposed stratified crusts (C1 and C2 areas) separated by a southeastward-dipping interface.

els of profile NCISP-2 and NCISP-4 (Zheng TY et al., 2005, 2006, 2009). The profile is characterized by a horizontally layered crust with a thick sedimentary cover (Figure 7a), and a thin crust with the thickness of ~30 km in the eastern part of the crust section, which represent a crust deformed by extension. In the western part of the crustal section the intra-crustal interfaces and the Moho are relatively smooth, with a Moho depth of ~40 km, which may represent a relatively stable tectonic feature in the NCC. The imaging from the central part of the crust section exhibits flexural intra-crustal interfaces, dipping and flat low-velocity zones, and a crustal root with the depth of 46 km, which was speculated to represent the tectonic remnant of the continental collision during the Paleoproterozoic assembly of the NCC (Zheng TY et al., 2009). The significant structural contrast between the eastern and western parts of the crust indicates that the craton destruction was mainly concentrated in the eastern NCC.

Seismic observations and imaging of typical profiles provide important evidence that the eastern NCC experienced strong extensional tectonism. In the northeastern margin of the NCC, an area with strong magmatism and well-developed metamorphic core complexes, the shear wave velocity image derived from the Dandong-Dongwu seismic profile (NCISP-6) across the northern edge of NCC and Central Asian Orogenic Belt (Figure 8) shows a distinct large-volume low-velocity anomaly at middle to lower crustal levels, with velocities that decrease with depth (Zheng TY et al., 2015). The unusual crustal fabrics provide strong constraints and important information regarding crustal transformations in a back-arc tectonic setting. Combining petrological data, geochemical data, and isotopic dating results, Zheng TY et al. (2015) suggested that mantle-derived magmatism induced melting and weakening of the crust. Movement and extension of the weakened crustal materials induced the heavy residue subsequently sank into the mantle. This physicochemical process is responsible for modifying the composition and structure of the crust.

5. Discussions and Conclusions

Seismic observations covering the entire NCC provide basic data for probing the crust structure of the NCC. We constructed a digital 3D crust and mantle velocity model VMNC and published it online (http://www.craton.cn/data [2017-03-01]). This study presents the results on crustal structures in the VMNC. This database has been used to review and analyze the seismic velocity structure of the crust, including the topography of the depth to basement and Moho, and the structural feature of typical tectonic profiles. The model of each tectonic setting shows significant variation in depth to Moho, thickness of cover and crustal internal structure, essentially controlled by the latest tectono-thermal processes. The analysis of the crustal structure based on the new database C-VMNC and illustrated in this paper indicates the following:

(1) The delimited area by the shallowing Moho in the eastern NCC represents the spatial range of the cratonic destruction.

(2) The east-west trend of observed variation of Moho depth in the NCC indicates that the present structure of the NCC crust retains the tectonic information of craton destruction during the Late Mesozoic to Cenozoic. The significantly variable basin structures in the eastern NCC indicate crustal modification by extension. Large-scale low-velocity anomalies appear in the crust of the eastern NCC, especially in the lower crust, indicating re-melting and weakening of the crust by magmatism.

(3) The structural pattern of east-west partition also implies that the tectonic activities of the craton destruction have modified the crustal structures at the northern and the southern margin of the NCC. The structural pattern, that a graben system with various shallow structures surrounding an ancient stable craton terrene, suggested a difference in shallow tectonic evolution in the Cenozoic time after craton destruction.

(4) The relatively smooth intra-crustal interfaces and the Moho and a Moho depth of ~40 km in the interior of the Ordos terrene may represent a relatively stable tectonic feature in the NCC. The crustal root beneath the northeastern Ordos terrene is considered as a tectonic remnant of the continental collision during the Paleoproterozoic assembly of the NCC. The thickened crust of ~ 60 km in the southwest of the Ordos can be ascribed to the re-

sponse to the lateral expansion of the northeastern Tibetan Plateau during the Cenozoic.

Acknowledgments

We gratefully acknowledge the researchers at the Seismic Array Laboratory, Institute of Geology and Geophysics, Chinese Academy of Sciences, and the Data Management Centre of the China National Seismic Network at the Institute of Geophysics, China Earthquake Administration, and Prof. Chunyong Wang for their efforts in collecting the data. This work was supported by the National Nature Science Foundation of China (Grant Numbers 91414301, 91014006).

References

Darby, B. J., Davis, G. A., Zhang, X. H., Wu, F. Y., Wilde, S. A., and Yang, J. H. (2004). The newly discovered Waziyu metamorphic core complex, YiwulüShan, western Liaoning Province, northwest China. *Earth Sci. Front.*, *11*, 145-155. https://doi.org/10.3321/j.issn:1005-2321.2004.03.016

Duan, Y. H., Liu, B. J., Zhao, J. R., Liu, B. F., Zhang, C. K., Pan, S. Z., Lin, J. Y., and Guo, W. B. (2015). 2-D P-wave velocity structure of lithosphere in the North China tectonic zone: Constraints from the Yancheng-Baotou deep seismic profile. *Sci. China Earth Sci.*, *58*, 1577-1591. https://doi.org/10.1007/s11430-015-5081-y

Duan, Y. H., Wang, F. Y., Zhang, X. K., Lin, J. Y., Liu, Z., Liu, B. F., Yang, Z. X., Guo, W. B., and Wei, Y. H. (2016). Three-dimensional crustal velocity structure model of the middle-eastern North China Craton (HBCrust1.0). *Sci. China Earth Sci.*, *59*, 1477-1488. https://doi.org/10.1007/s11430-016-5301-0

Fan, W., and Menzies, M. A. (1992). Destruction of aged lower lithosphere and accretion of asthenosphere mantle beneath eastern China. *Geotecton. Metallog.* (*in Chinese*), *16*, 171-180.

Guo, J. H., Peng, P., Chen, Y., Jiao, S. J., and Windley, B. F. (2012). UHT sapphirine granulite metamorphism at 1.93-1.92 Ga caused by gabbronorite intrusions: implications for tectonic evolution of the northern margin of the North China Craton. *Precambrian Res*, *222-223*, 124-142. https://doi.org/10.1016/j.precamres.2011.07.020

Jia, S. X., Wang, F. Y., Tian, X. F., Duan, Y. H., Zhang, X. K., Liu, B. F., and Lin, J. Y. (2014). Crustal structure and tectonic study of North China Craton from a long deep seismic sounding profile. *Tectonophysics*, *627*, 48-56. https://doi.org/10.1016/j.tecto.2014.04.013

Liu, D. Y., Nutman, A. P., Compston, W., Wu, J. S., and Shen, Q. H. (1992). Remnants of ≥3800 Ma crust in the Chinese part of the Sino-Korean craton. *Geology*, *20*, 339-342. https://doi.org/10.1130/0091-7613(1992)020<0339:ROMCIT>2.3.CO;2

Liu, L. H., Hao, T. Y., Lü, C. C., You, Q. Y., Pan, J., Wang, F. Y., Xua, Y., Zhao, C. L., and Zhang, J. S. (2015). Crustal structure of Bohai Sea and adjacent area (North China) from two onshore–offshore wide-angle seismic survey lines. *J. Asian Earth Sci.*, *98*, 457-469. https://doi.org/10.1016/j.jseaes.2014.11.034

Liu, M. J., Mooney, W. D., Li, S. L., Okaya, N., and Detweiler, S. (2006). Crustal structure of the northeastern margin of the Tibetan Plateau from the Songpan-Ganzi terrane to the Ordos basin. *Tectonophysics*, *420*, 253-266. https://doi.org/10.1016/j.tecto.2006.01.025

Meng, Q. R., and Zhang, G. W. (2000). Geologic framework and tectonic evolution of the Qinling orogen, central China. *Tectonophysics*, *323*, 183-196. https://doi.org/10.1016/S0040-1951(00)00106-2

Menzies, M. A., Fan, W. M., and Zhang, M. (1993). Palaeozoic and Cenozoic lithoprobes and the loss of >120 km of Archaean lithosphere, Sino-Korean craton, China. *Geol. Soc. Lond. Special Publicat.*, *76*, 71-78. https://doi.org/10.1144/GSL.SP.1993.076.01.04

Metcalfe, I. (2011). Tectonic framework and Phanerozoic evolution of Sundaland. *Gondwana Res.*, *19*, 3-21. https://doi.org/10.1016/j.gr.2010.02.016

Peng, P., Wang, X. P., Windley, B. F., Guo, J. H., Zhai, M. G., and Li, Y. (2015). Spatial distribution of 1950-1800 Ma metamorphic events in the North China Craton: implications for tectonic subdivision of the craton. *Lithos*, *202-203*, 250-266. https://doi.org/10.1016/j.lithos.2014.05.033

Qiu, R. Z., Li, T. D., Deng, J. F., Zhou, S., Li, J. F., Xiao, Q. H., Wu, Z. X., and Zhao, G. C. (2004). Crust-mantle petrological and petrochemical structures of three kinds of lithospheres in North China and their continental dynamic implications. *Acta Patrol. Mineral.* (*in Chinese*), *23*, 127-140. https://doi.org/10.3969/j.issn.1000-6524.2004.02.004

Ren, J. Y., Tamaki, K., Li, S. T., and Zhang, J. X. (2002). Late Mesozoic and Cenozoic rifting and its dynamic setting in Eastern China and adjacent areas. *Tectonophysics*, *344*, 175-205. https://doi.org/10.1016/S0040-1951(01)00271-2

Wang, C. Y., Sandvol, E., Zhu, L., Lou, H., Yao, Z. X., and Luo, X. H. (2014). Lateral variation of crustal structure in the Ordos block and surrounding regions, North China, and its tectonic implications. *Earth Planet. Sci. Lett.*, *387*, 198-211. https://doi.org/10.1016/j.epsl.2013.11.033

Wang, H. Z., and Mo, X. X. (1995). An outline of the tectonic evolution of China. *Episodes*, *18*, 6-16.

Wu, F. Y., Lin, J. Q., Wilde, S. A., Zhang, X. O., and Yang, J. H. (2005). Nature and significance of the Early Cretaceous giant igneous event in eastern China. *Earth Planet. Sci. Lett.*, *233*, 103-119. https://doi.org/10.1016/j.epsl.2005.02.019

Xiao, W. J., Windley, B. F., Hao, J., and Zhai, M. G. (2003). Accretion leading to collision and the Permian Solonker suture, Inner Mongolia, China: termination of the Central Asian orogenic belt. *Tectonics*, *22*, 1069. https://doi.org/10.1029/2002TC001484

Zhai, M. G., and Santosh, M. (2011). The early Precambrian odyssey of the North China Craton: A synoptic overview. *Gondwana Res.*, *20*, 6-25. https://doi.org/10.1016/j.gr.2011.02.005

Zhai, M. G. (2008). Lower crust and lithospheric mantle beneath the North China Craton before the Mesozoic lithospheric disruption. *Acta Petrol. Sin.* (*in Chinese*), *24*, 2185-2204.

Zhang, J. H., and Zheng, T. Y. (2015). Receiver function imaging with reconstructed wavefields from sparsely scattered stations. *Seismol. Res. Lett.*, *86*, 165-172. https://doi.org/10.1785/0220140028

Zhao, G. C., Wilde, S. A., Cawood, P. A., and Sun, M. (2001). Archean blocks and their boundaries in the North China Craton: Lithological, geochemical, structural and P-T path constraints and tectonic evolution. *Precambrian Res.*, *107*, 45-73. https://doi.org/10.1016/S0301-9268(00)00154-6

Zheng, T. Y., Zhao, L., and Chen, L. (2005). A detailed receiver function image of the sedimentary structure in the Bohai Bay Basin. *Phys. Earth Planet. Inter.*, *152*, 129-143. https://doi.org/10.1016/j.pepi.2005.06.011

Zheng, T. Y., Chen, L., Zhao, L., Xu, W. W., and Zhu, R. X. (2006). Crust-mantle structure difference across the gravity gradient zone in North China Craton: Seismic image of the thinned continental crust. *Phys. Earth Planet. Inter.*, *159*, 43-58. https://doi.org/10.1016/j.pepi.2006.05.004

Zheng, T. Y., Zhao, L., Xu, W. W., and Zhu, R. X. (2008). Insight into modification of North China Craton from seismological study in the Shandong Province. *Geophys. Res. Lett.*, *35*, L22305. https://doi.org/10.1029/2008GL035661

Zheng, T. Y., Zhao, L., and Zhu, R. X. (2009). New evidence from seismic imaging for subduction during assembly of the North China craton. *Geology*, *37*, 395-398. https://doi.org/10.1130/G25600A.1

Zheng, T. Y., Yang, J. H., He, Y. M., and Zhao, L. (2015). Seismological constraints on the crustal structures generated by continental rejuvenation in northeastern China. *Sci. Rep.*, *5*, 14995. https://doi.org/10.1038/srep14995

Zheng, X. F., Yao, Z. X., Liang, J. H., and Zheng, J. (2010). The role played and opportunities provided by IGP DMC of China National Seismic Network in Wenchuan earthquake disaster relief and researches. *Bull. Seismol. Soc. Am.*, *100*(5B), 2866-2872. https://doi.org/10.1785/0120090257

Zhu, R. X., Xu, Y. G., Zhu, G., Zhang, H. F., Xia, Q. K., and Zheng, T. Y. (2012). Destruction of the North China craton. *Sci. China Earth Sci.*, *55*, 1565-1587. https://doi.org/10.1007/s11430-012-4516-y